Tropospheric products from high-level GNSS processing in Latin America

M. V. Mackern (1,2,3); M. L. Mateo(2,3); M. F. Camisay (2,3); P. V. Morichetti(3)

(1) Consejo Nacional de Investigaciones Científicas y Técnicas (Argentina); (2) Facultad de Ingeniería. Universidad Nacional de Cuyo (Argentina); (3) Facultad de Ingeniería. Universidad Juan A. Maza (Argentina)

Introduction

Integrated Water Vapour (IWV) plays a fundamental role in several weather processes that deeply influence human activities. Retrieving IWV content in the atmosphere can be performed in different ways using independent techniques: the more traditional ones like radiosondes and ground-based microwave radiometers, up to the more recent ones based on satellite techniques. In particular, the GNSS-based tropospheric Zenith Total Delay (ZTD) estimates allow inferring IWV values with high accuracy.

In our study, we concentrate on the estimation of IWV in Latin America using as input data the ZTD values obtained in (1) the operational processing of the regional reference frame SIRGAS (Sistema de Referencia Geocéntrico para las Américas), and (2) the generation of near real-time products applying the Precise Point Positioning (PPP) approach. To assess the reliability of our results (ZTD and IWV values), they are compared with the operational IGS products (ZTD_{IGS}) and estimations inferred from radiosonde profiles (ZTD_{RS}, IWV_{RS}).

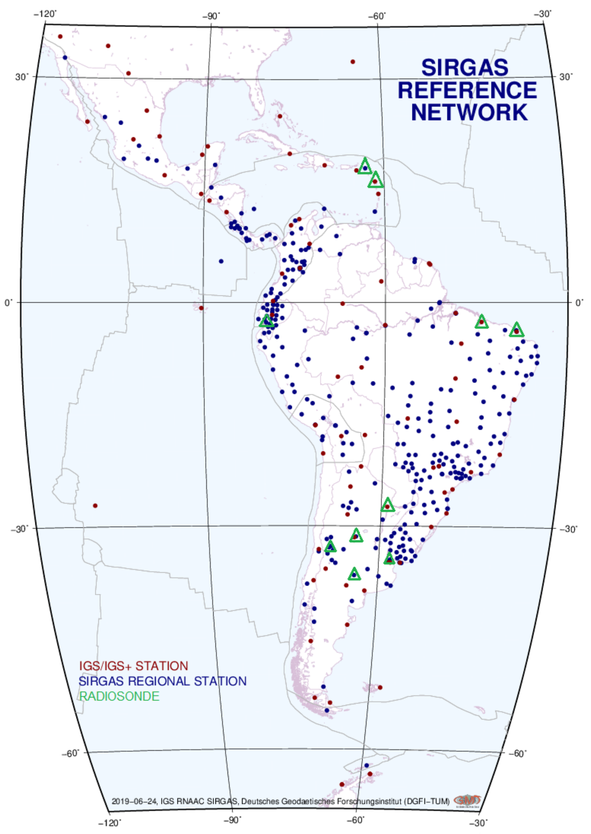

Fig. 1: SIRGAS GNSS stations and radiosonde sites considered in this study.

Estimation of ZTD values based on the operational SIRGAS processing (ZTD_{SIR})

SIRGAS is at present given by a network of about 400 continuously operating GNSS stations (Fig. 1). These stations are routinely processed by ten SIRGAS Analysis Centres (AC) following the IERS standards and the most-recent GNSS processing guidelines issued by the IGS. The ZTD is modelled using the Global Mapping Function (GMF, Böhm et al., 2006). A-priori zenith hydrostatic delay (ZHD) values are derived from gridded coefficients based on the Global Pressure Temperature (GPT) model (Böhm et al., 2007) and are refined by computing zenith wet delays (ZWD) in a 1-hour interval using the Vienna Mapping Function (VMF, Böhm et al., 2006). In addition, horizontal gradient parameters are estimated using the model described by Chen and Herring (1997). As each SIRGAS-AC processes a different sub-network of SIRGAS stations, we perform a combination of the ZTD estimates delivered in the individual solutions by means of a weighed least-squares adjustment using the inverse of the input data variances as a weighting factor. Our empirical experiments cover five years (Jan 2014 to Dec 2018) and are based on ZTD estimates provided by the SIRGAS-AC using the Bernese GNSS Software V5.2 (BSW52, Dach et al. 2015), see Table 1.

For validation, our results are compared with the operational IGS products (ZTD_{IGS}) and ZTD values calculated from radiosonde profiles (ZTD_{RS}). In the latter, the ZTD values are determined following Askne and Nordius (1987), see Fig. 2. The mean temperature of the atmosphere (Tm) and the pressure at the GNSS stations (P_{GNSS}) are inferred from radiosonde profiles data (temperature and dew-point) obtained at the Wyoming Weather Web, University of Wyoming. The ZHD_{RS} values are obtained after Davis et al. (1985).

Our results present a quite good agreement with the IGS products (see Figs. 3 and 4). Discrepancies between both estimates obtained at 15 stations present a mean RMS value of ±6.8 mm (0.29 % of the mean ZTD) with a negative mean bias of 1.5 mm(0.07 % of the mean ZTD) . The comparison with ZTD_{RS} is also very promising: discrepancies computed at ten radiosonde stations (see Fig. 1) have a mean RMS of 7.5 mm (0.32 % of the mean ZTD) and a negative mean bias of 2 mm (0.09 % of the mean ZTD).

ZTD estimation applying PPP (ZTD_{PPP})

The objective of applying PPP is the determination of ZTD and IWV values in near real-time. Therefore, we selected as case of study two epochs presenting strong storms in the central-western region of South America:

Case 1: Feb 21 - Mar 27, 2016; 10 stations
Case 2: Aug 12 - Aug 27, 2018; 15 stations

The ZTD_{PPP} values are estimated using BSW52 and the BKG NTRIP Client (BNC) software (Weber et al. 2016). Table 2 summarizes the input data, models, and main configuration used for each software. ZTD_{PPP} values estimated using both BSW52 and BNC are compared with the corresponding ZTD_{SIR} values. The BSW52-based estimates show a better agreement than the BNC-based estimates (see Table 3 and Figs. 5 and 6). This is most probably a consequence of the fact that ZTD_{SIR} and the BSW52-based ZTD_{PPP} use the same models to determine the tropospheric parameters.

Table 1: SIRGAS Analysis Centres

CEPGE	Centro de Procesamiento de Datos GNSS del Ecuador, Instituto Geográfico Militar (Ecuador), BWS52, 139 stations
CNPDG-UNA	Centro Nacional de Procesamiento de Datos GNSS, Universidad Nacional (Costa Rica), BWS52, 85 stations
CPAGS-LUZ	Centro de Procesamiento y Análisis GNSS SIRGAS de la Universidad del Zulia (Venezuela), BWS52, 103 stations
IBGE	Instituto Brasileiro de Geografia e Estatistica (Brazil), BWS52, 221 stations
IGAC	Instituto Geográfico Agustín Codazzi (Colombia), BWS52, 99 stations
IGM-Cl	Instituto Geográfico Militar (Chile), BWS52, 140 stations
IGN-Ar	Instituto Geográfico Nacional (Argentina), GAMIT, 137 stations
INEGI	Instituto Nacional de Estadística y Geografía (México), GAMIT, 59 stations
IGM-Uy	Instituto Geográfico Militar (Uruguay), BWS52, 129 stations
IGS RNAAC SIRGAS	Deutsches Geodätisches Forschungsinstitut, Technischen Universität München, (Germany), BWS52, 170 stations

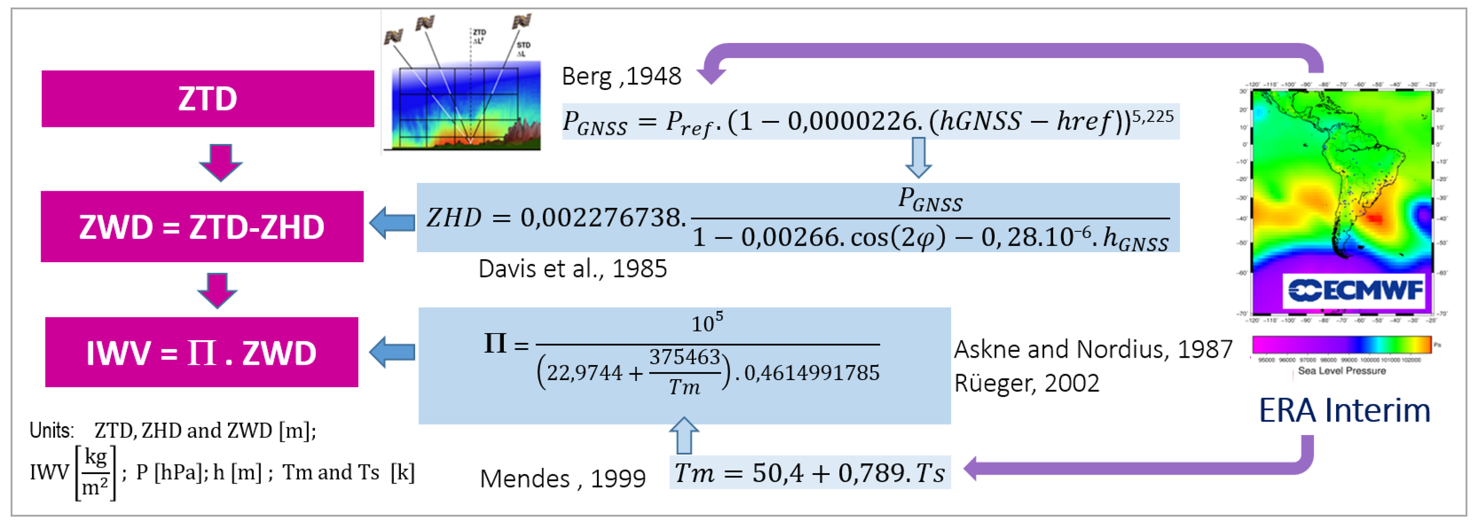

Fig. 2: Strategy for the estimation of IWV from GNSS-based ZTD values.

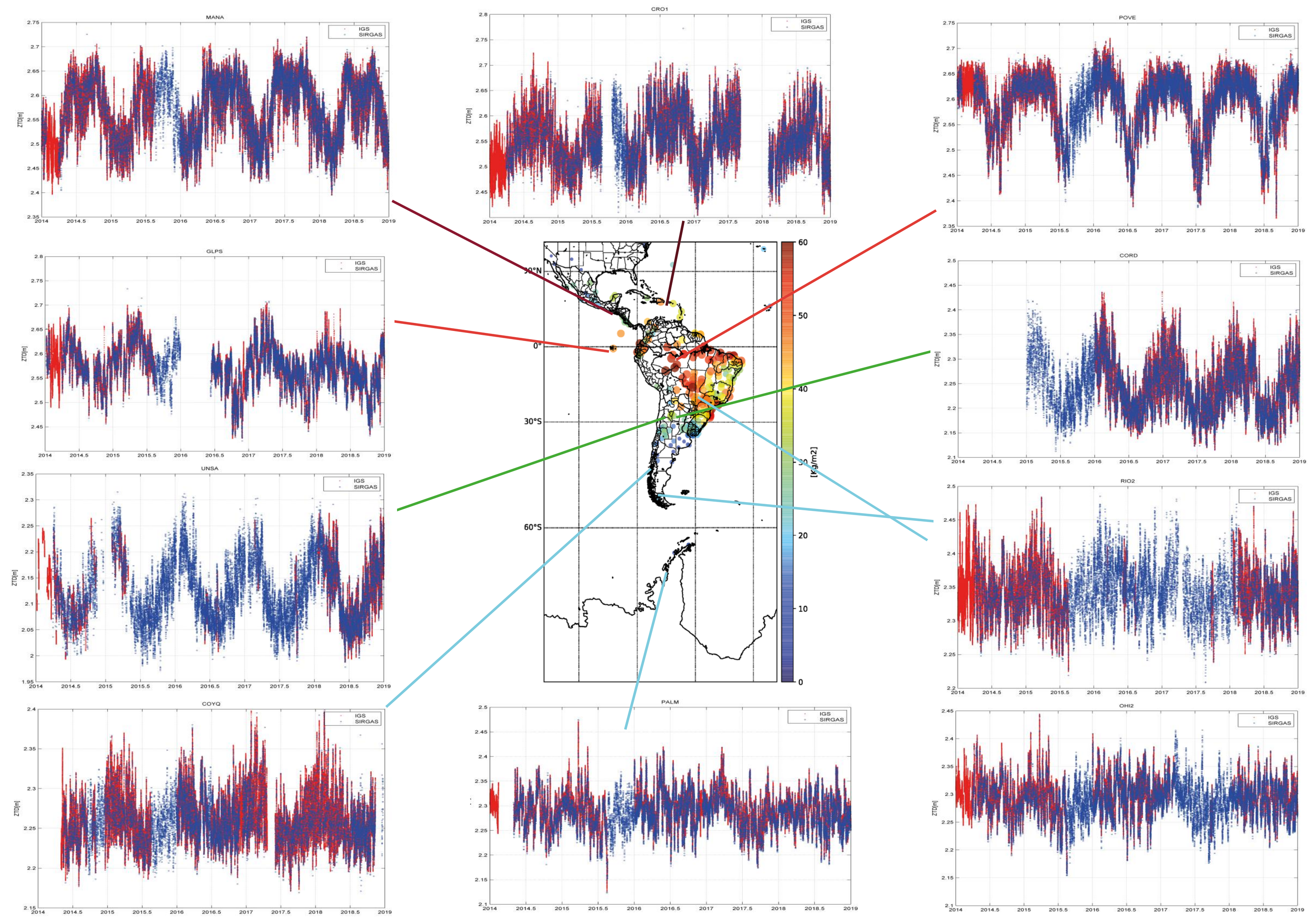
Fig. 3: Time series of ZTD_{SIR} (blue) and ZTD_{IGS} (red) values at selected SIRGAS stations (Jan 2014 – Dec 2018).

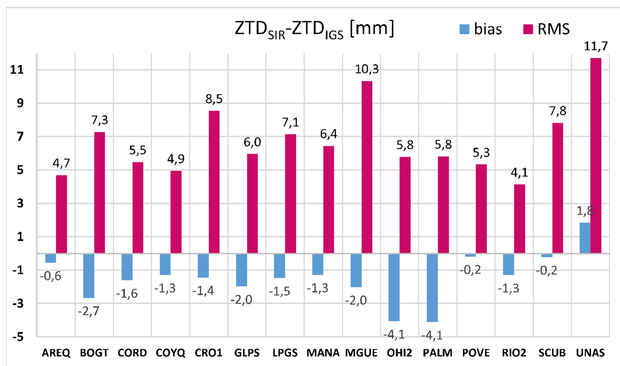

Fig. 4: Comparison of ZTD_{SIR} and ZTD_{IGS} values at selected SIRGAS stations (Jan 2014 – Dec 2018).

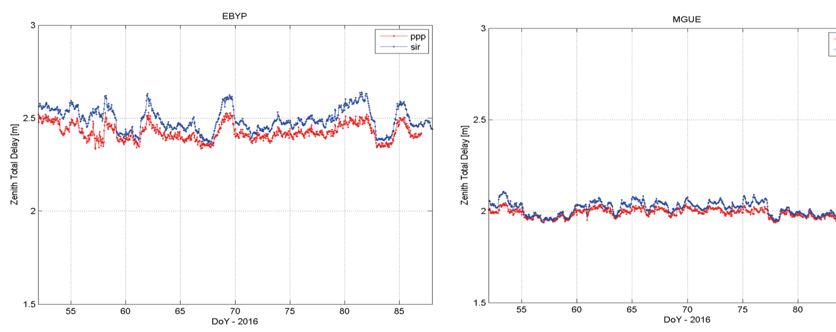
Fig. 5: Comparison of ZTD_{SIR} and BWS52-based ZTD_{PPP} values at two selected SIRGAS stations.

Table 2: Input data, models and basic configuration for the estimation of ZTD values within the operational SIRGAS processing and using the Precise Point Positioning (PPP) approach.

		Operational SIRGAS Processing	Precise Point Positioning	
Software		Bernese v5.2	BNC	Bernese v5.2
Observations		GPS+GLONASS	GPS+GLONASS	GPS
Sampling interval		30 seconds	real time streams (1 s)	RINEX (1 s)
Orbits and EOP		Final IGS products igswwwwD.sp3 Igswwww7.erp	Broadcast + IGS03 correction	Rapid (CODE) CODEwwwwD.EPH CODEwwwwD.ERP
Clock correction			IGS03 stream correction	Rapid (CODE) CODEwwwwD.CLK
Troposphere modeling	A-priori	GMF and VMF (Böhm et al., 2006)	Saastamoinen (1973) dT / cos(z)	GMF (Böhm et al., 2007)
	Parameter estimation	VMF + Gridded VMF1 coefficients (00, 06 12 and 18 UTC)	Saastamoinen dT / cos(z)	VMF + Gridded VMF1 coefficients (00, 06 12 and 18 UTC)
	Horizontal gradients	CHENHER Model Chen and Herring (1997)	no	no
	Spacing	1 or 2 hours	same as observation	1 h

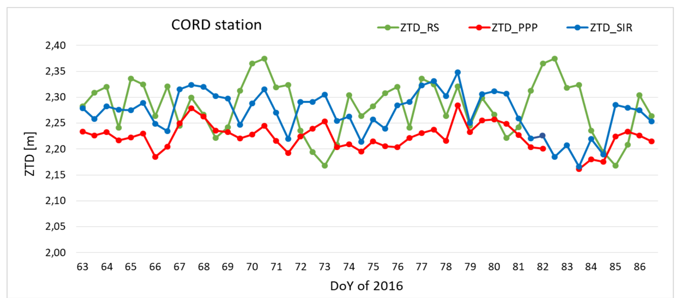

Fig. 6: Comparison of ZTD_{SIR} , BWS52-based ZTD_{PPP} and ZTD_{RS} values at a GNSS station located in Cordoba (Argentina).

Table 3: Comparison of ZTD values based on the operational SIRGAS processing (ZTD_{SIR}) and PPP estimates using BSW52 and BNC (45 days, 10 stations)

Software	Bias [cm]	RMS [cm]
BWS52	5.2 (2 % of the ZTD)	0.016
BNC	12.1 (5 % of the ZTD)	12.900

Determination of IWV values from GNSS-based ZTD estimates

The GNSS-based ZTD values are used to calculate the IWV applying the ratio of Askne and Nordius (1987) to the wet component of the delay (ZWD), see Fig. 2. ZTD stands in general for ZTD_{SIR} or ZTD_{PPP}. ZWD values are obtained by removing the zenith hydrostatic delay (ZHD), which is calculated according to Davis et al. (1985). Sea level pressure values (P_{ref}) are extracted from the ERA-Interim products provided by ECMWF and are reduced to the height of the GNSS stations (P_{GNSS}) following Berg (1948). For the factor Π, the weighted mean temperature of the atmosphere (*Tm*) is calculated in accordance with Mendes (1999) using the surface temperature (*Ts*) also provided by ERA-Iterim. The values for the refractivity constants are taken from Rüeger (2002). Following this strategy, we generate four daily IWV maps (at 00:00, 06:00, 12:00 and 18:00 UTC) for the entire SIRGAS region, see some examples in Fig. 7.

Figures 8 and 9 show the comparison of IWV_{SIR} (inferred from ZTD_{SIR}) values with values obtained from radiosonde profiles (IWV_{RS}) at the Wyoming Weather Web, University of Wyoming, for selected SIRGAS stations. The correlation coefficient of the two series presented in Fig. 8 is 0.94, which indicates a very good agreement between both estimates. In the other hand, the comparison IWV_{PPP} (calculated from the BWS52-based ZTD_{PPP} values) with IWV_{RS} produces discrepancies with a mean RMS of 1 kg/m^2 and a bias of 2,37 kg/m^2.

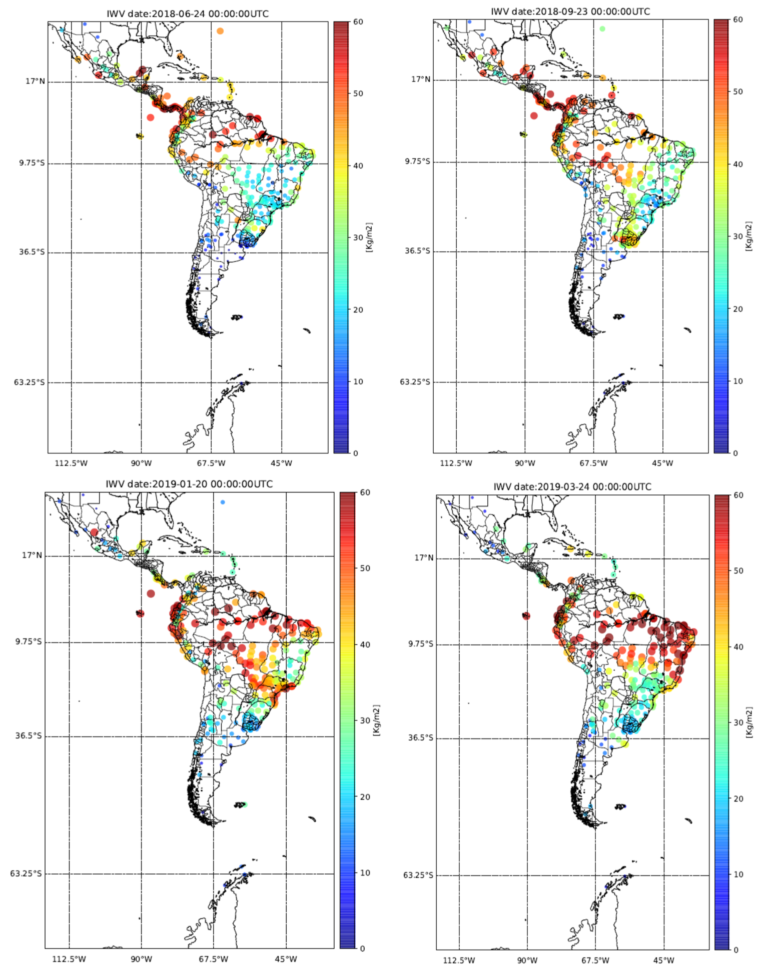
Fig. 7: Maps of IWV inferred from the ZTD estimates produced within the operational SIRGAS processing.

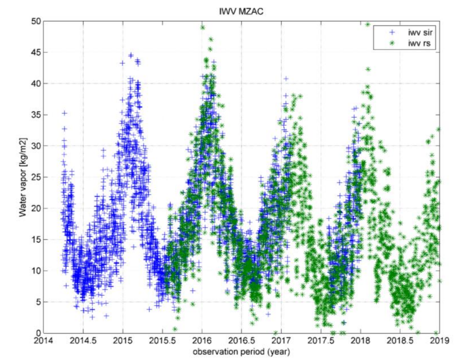
Fig. 8: Time series of IWV values inferred from GNSS-based ZTD estimates (IWV_{SIR}) and radisonde profile data (IWV_{RS}) in Mendoza (Argentina).

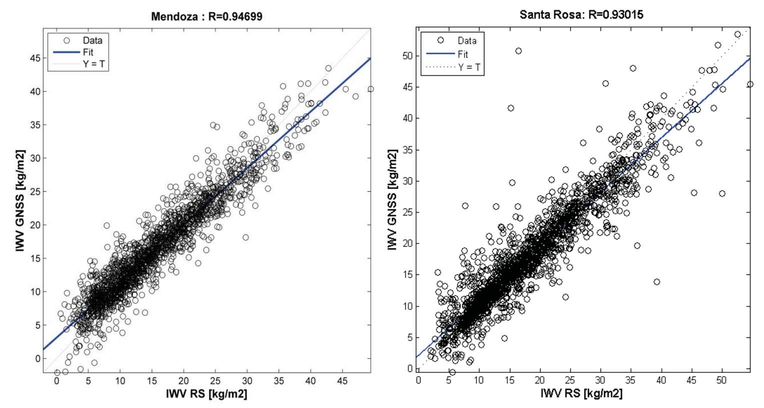

Fig. 9: Scatter plot comparing IWV values inferred from GNSS-based ZTD estimates (IWV_{SIR}) and radiosonde profile data (IWV_{RS}) at two selected SIRGAS stations (Jan 2014 to Dec 2018).

Final remarks and outlook

Our experiments demonstrates that we are able to determine ZTD and IWV values with a high reliability over Latin America. The primary input data is provided by the infrastructure (stations and analysis centres) of the regional reference frame SIRGAS. This support is deeply acknowledged. The challenges for the future are (1) to develop algorithms of prediction to generate surface maps based on the pointwise estimations and (2) to implement the automatized computation of ZTD and IWV models. The objective is the routine publication of these products within SIRGAS to provide reliable data for atmospheric research at national and regional levels.

References

Askne J, Nordius H (1987). Estimation of tropospheric delay for microwaves from surface weather data, Radio Sci., 22, 379–386, https://doi:10.1029/RS022i003p00379.
Berg H 1948. Allgemeine meteorologie. Dümmler's Verlag, Bonn (in German).
Böhm J, Werl B, Schuh H (2006). Troposphere mapping functions for GPS and very long baseline interferometry from European Centre for Medium-Range Weather Forecasts operational analysis data, J. Geophys. Res., 111, B02406; https://doi.org/10.1029/2005JB003629.
Boehm J, Heinkelmann R, Schuh H (2007). Short Note: A global model of pressure and temperature for geodetic applications J Geod 81: 679. https://doi.org/10.1007/s00190-007-0135-3
Chen G, Herring TA (1997). Effects of atmospheric azimuthal asymmetry on the analysis of space geodetic data, J. Geophys. Res., 102(B9): 20489-20502; https://doi.org/10.1029/97JB01739
Dach R, Lutz S, Walser P, Fridez P (2015). Bernese GNSS Software Version 5.2. Astronomical Institute, University of Bern, Bern. ISBN: 978-3-906813-05-9 ; Open Publishing. DOI: 10.7892/boris.72297
Davis JL, Herring TA, Shapiro II, Rogers AEE, Elgered G (1985). Geodesy by radio interferometry: effects of atmospheric modeling errors on estimates of baseline length. Radio Sci 20(6):1593–1607
Mendes VB (1999). Modeling the Neutral-Atmosphere Propagation Delay in Radiometric Space Techniques, (Ph.D. dissertation). Department of Geodesy and Geomatics Engineering Technical Report No 199, Univ. of New Brunswick, Canada
Rüeger JM (2002). Refractive index formula for radio waves, Proc. XXII FIG Int. Congr., April 19-26, 2002, available from: http://www.fig.net/resources/proceedings/fig_proceedings/fig_2002/Js28/JS28_rueger.pdf
Saastamoinen J (1973) Contribution to the Theory of Atmospheric Refraction. Bulletin Géodésique, 107, 13-34. http://dx.doi.org/10.1007/BF02522083
Weber G, Mervart L, Stürze A, Rülke A, Stöcker D (2016). BKG Ntrip Client, Version 2.12. Mitteilungen des Bundesamtes für Kartographie und Geodäsie, Vol. 49, Frankfurt am Main.

27th IUGG General Assembly, July 8 - 18, 2019, Montreal, Canada